JOURNAL OF MATERIALS SCIENCE **36** (2001) 1931–1938

Room temperature creep and strain-rate-dependent stress-strain behavior of pipeline steels

SHENG-HUI WANG, YONGGANG ZHANG*, WEIXING CHEN
Department of Chemical and Materials Engineering, University of Alberta, Edmonton, Alberta, Canada T6G 2G6
E-mail: weixing.chen@ualberta.ca

Creep deformation and the effect of strain-rate on stress-strain behavior of X-52, X-70 and X-80 pipeline steels at room temperature were studied using round tension test specimens. Depending on its chemical composition and the processing condition (as-received or fully annealed), a pipeline steel may exhibit a stress-strain curve with or without a yield point. The as-received and the annealed steels with both type of yielding behavior were creep tested at a constant stress either below or past the yield point / 0.2% offset yield strength. Independent of yielding behavior, significant post-yield creep deformation was observed in all the steels. The pre-yield creep, however, is strongly dependent on the yielding behavior. In the presence of a yield point, only a minor deformation was detected in the steels subject to the pre-yield creep. In the absence of a yield point, pre-yield creep deformation occurred to a relatively large extent. For the latter case, an annealing treatment further enhanced creep deformation. A strain-rate-dependent stress-strain behavior was also observed in all the steels that show significant creep deformation. Dislocation mechanisms responsible for the creep behavior observed in the study are also provided in the paper.

1. Introduction

Room temperature creep deformation often causes significant technical problems to structures in service. The stress relaxation due to creep deformation, for example, is one of the major concerns over the reliability of high strength steel wire for building applications [1]. For underground pipeline steels, the susceptibility to stress-corrosion cracking (SCC) is of great interest. Depending on the corrosion environment, creep deformation may affect SCC by causing local rupture of surface passivation film or by enhancing hydrogen diffusion through dislocation movement [2–5].

With few exceptions [6–8], where there is primary creep followed by a steady state creep, room temperature creep normally exhibits a work-hardening feature, with an eventual exhaustion of creep deformation due to lack of recovery [9]. A time-dependent dislocation glide is believed to be the characteristic of room temperature creep [10–12].

The room temperature creep deformation is found to depend on the magnitude of applied stress [3, 7, 9], and the metallurgical conditions of the material arising from thermal and thermal mechanical processing [1, 4, 7, 9, 13]. Although room temperature creep has been studied in number of alloys, many factors determining the creep deformation at room temperature remain unknown.

The purpose of this paper is to characterize the room temperature creep deformation and the strain-rate sensitivity of stress-strain behavior of pipeline steels in relation to processing conditions. Special attention is paid to the inter-correlation of creep deformation with various yielding behavior observed in the pipeline steels.

2. Materials and experimental procedure

X-52, X-70 and X-80 pipeline steels in the as-received (AR) and fully annealed (FA) conditions were used in the investigation. The chemical compositions of the steels are listed in Table I. The full annealing treatment was conducted at 820 °C (1 h) for X-52, 900°C (1 h) for X-70, and 820 °C (1.5 h) for X-80, followed by furnace cooling.

The tensile and creep tests were conducted using standard round tension specimens with a diameter of 6 mm and a length of 36 mm in the reduced section. The specimens were machined from the steel pipes such that the long dimension of the sample coincided either with the pipe longitudinal direction (for X-52 and X-70), or with the pipe circumferential direction (for X-80). All the tests were carried out on a closed loop servo-hydraulic testing machine (INSTRON 8516) in a temperature-controlled laboratory set at 22°C. Strain was measured using a strain gauge extensometer with a

*On leave from Department of Materials Science&Engineering, Beijing University of Aeronautics and Astronautics, Beijing, People's Republic of China.

TABLE I Chemical compositions (wt.%) of the steels used in this study

	C	N	Mn	P	Si	Cu	Ni	Cr	Mo	Cb	Ti	Al
X-52	0.07	<0.0015	0.80	0.016	0.27	0.28	0.09	0.05	<0.01	0.012	0.019	0.031
X-70	0.06	0.0040	1.80	0.006	0.39	0.26	0.30	0.04	0.302	0.083	0.017	0.042
X-80	0.06	0.0031	1.75	0.012	0.36	0.27	0.31	0.04	0.302	0.079	0.011	0.026

TABLE II Mechanical properties of the pipeline steels used in this study tested at a strain-rate of 10^{-3}/s

Steel	condition	YS (MPa)	UYS (MPa)	LYS (MPa)	S_u (MPa)	YPE (%)	El_u (%)	El_t (%)
X-52	AR	—	433.9	382.2	484.8	2.0	15.9	32.3
	FA	—	415.9	323.9	431.9	3.3	21.2	39.0
X-70	AR	566.8	—	—	649.2	—	6.8	17.6
	FA	306.4	—	—	516.0	—	18.8	31.5
X-80	AR	—	675.8	651.6	684.1	2.6	8.3	19.3
	FA	286.3	—	—	599.6	—	18.0	32.7

YS: Yield strength (offset 0.2%) YPE: Yield point elongation
UYS: Upper yield strength El_u: Uniform elongation
LYS: Lower yield strength El_t: Elongation (25 mm gage length)
S_u: Tensile Strength

gauge length of 25 mm, which was attached to the gauge section of the specimen with rubber bands. Each of the tests was computer-controlled using a built-in software (Instron Series IX Automated Materials Tester). The tensile tests were performed first under the strain control mode up to a strain of five percent, and then under displacement control until failure.

The creep tests were conducted under constant load, which were computer-controlled with the Instron WaveMaker-Runtime software. For pre-yield creep test, the creep stress, which was either below 0.2% yield strength or below the upper yield point, was applied to the test specimen via the load-control mode. For post-yield creep, the test sample was loaded to a stress in the plastic region via displacement control mode. For all the creep tests, the strain-rate in the process of loading was controlled to be approximately 1×10^{-2}/s. All the data were recorded by a computer. The dislocation structures of the thin foils from the samples tested were examined in JEOL 2000FX Analytical TEM/STEM (Transmission electron microscopy / Scanning transmission electron microscopy).

3. Experimental results

3.1. Stress-strain behavior and the influence of strain-rate

Fig. 1 compares the stress-strain curves of the steels tested at a strain-rate of 1×10^{-3}/s. The tensile properties are summarized in Table II. The influence of strain-rate on the stress-strain behavior of the steels is shown in Fig. 2 (in which only the initial portion of the stress-strain curves is presented).

For both the as-received and the annealed X-52 pipeline steels, the stress-strain curves exhibit a wide range of discontinuous yielding (Figs 1 and 2). The difference between the upper yield strength (UYS) and the lower yield strength (LYS) is quite significant (Table II). The annealing treatment has changed the mechanical properties of the X-52 steel slightly.

The as-received X-80 pipeline steel also exhibits a discontinuous yielding behavior. However, this feature

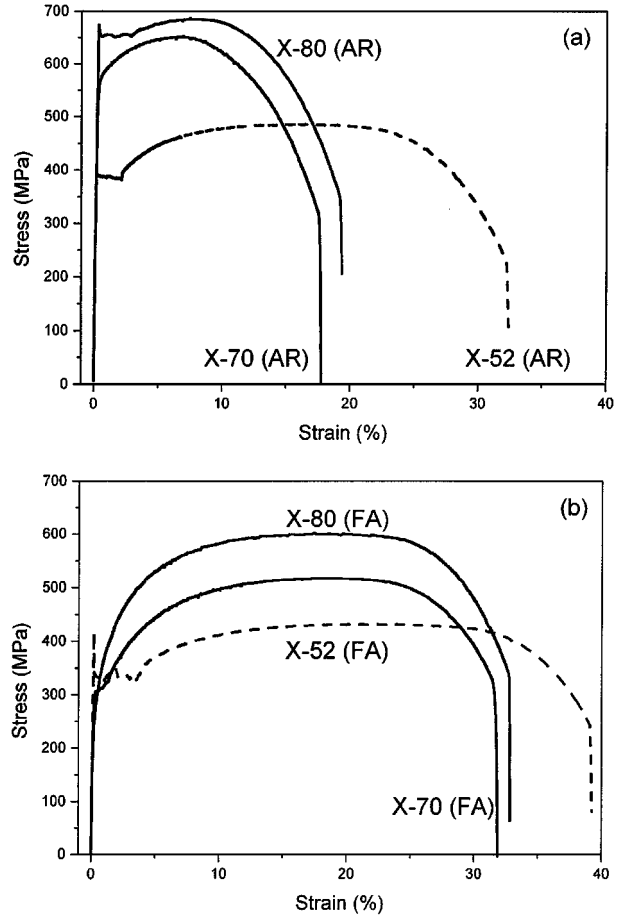

Figure 1 Engineering stress-strain curves of the pipeline steels: (a) as-received condition (AR); (b) fully annealed condition (FA).

is absent after the steel is fully annealed (Figs 1 and 2). The annealing treatment has sharply reduced the yield strength and enhanced the ductility of the material. In addition, the annealed steel has experienced strong work-hardening effect during tensile testing in comparison with the as-received material.

X-70 pipeline steel does not exhibit the discontinuous yielding behavior in either the as-received or the

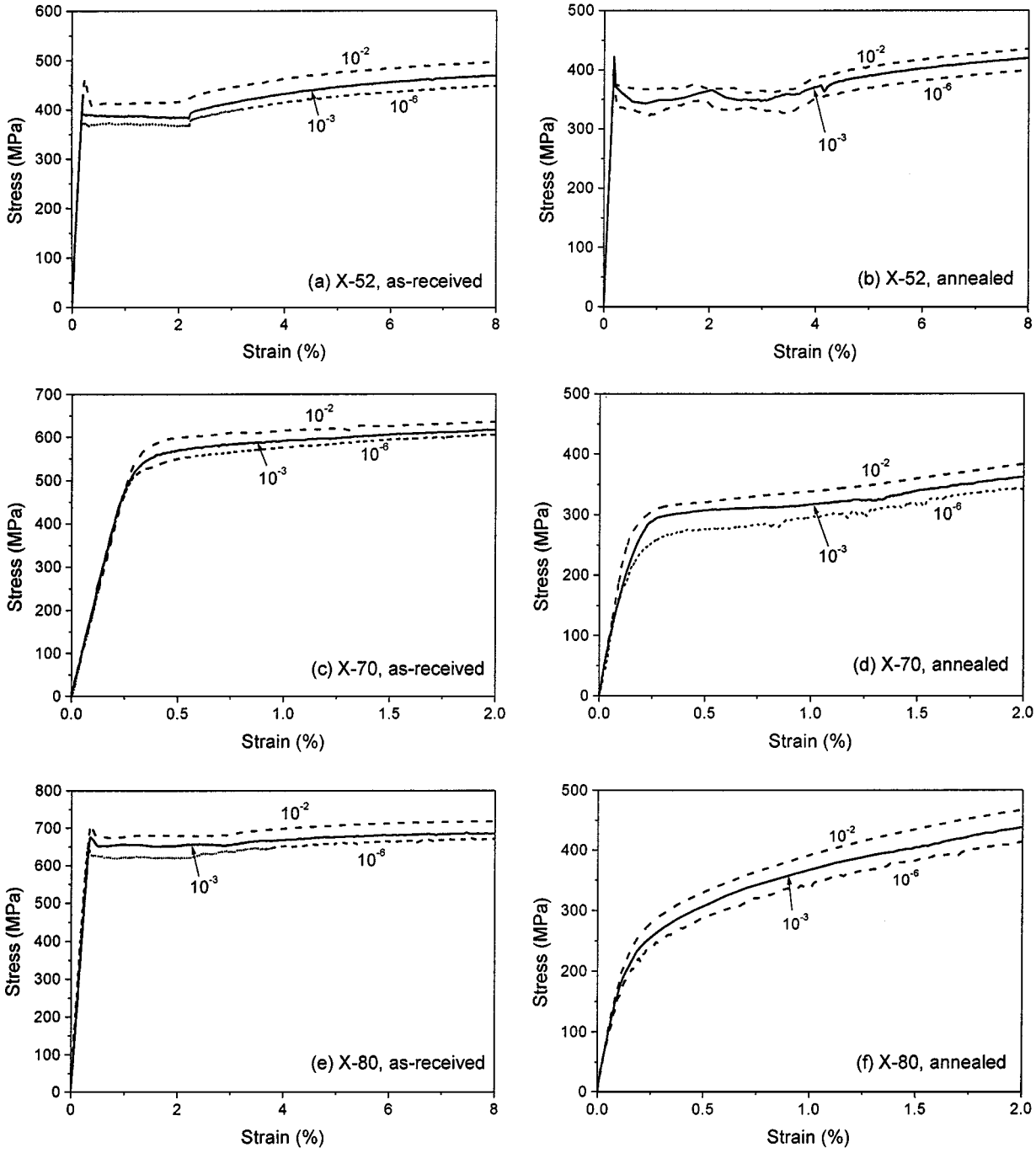

Figure 2 Stress-strain behavior of the pipeline steels tested at three different strain-rates.

annealed conditions (Figs 1 and 2). Similar to X-80, the X-70 steel after annealing treatment also shows a significant reduction in yield strength, and an increase in elongation. The work-hardening effect is also quite strong in annealed X-70.

Strain-rate appears to have little effect on the pre-yield stress-strain behavior of those steels whose stress-strain curves exhibit a yield point (Fig. 2a,b and e). After yielding, however, the tensile stress is seen to increase with strain-rate. For some of the stress-strain curves which are free of yield points, the influence of strain-rate on the stress-strain behavior starts in the region far below the 0.2% yield strength (Fig. 2d and f). In these stress-strain curves, a higher strain-rate also results in a higher strength in the plastic region (Fig. 2c, d and f).

3.2. Creep behavior

Figs 3–7 show the pre-yield creep curves of the three pipeline steels tested at various stress levels (expressed as percentage of yield strength or upper yield strength). From these creep curves, it can be seen that the pre-yield creep exhibits a feature of work-hardening. The creep rate is relatively high at the beginning, and it decreases with time until a saturated stage where no further deformation takes place. Higher creep stress results in a larger saturated creep strain (Figs 3–7). No significant creep deformation is seen in the sample that was pre-crept and reloaded to the initial creep stress (Fig. 8).

In the above creep tests, the saturated creep strain is strongly dependent on the yielding behavior of the steels. For both the as-received and the annealed steels

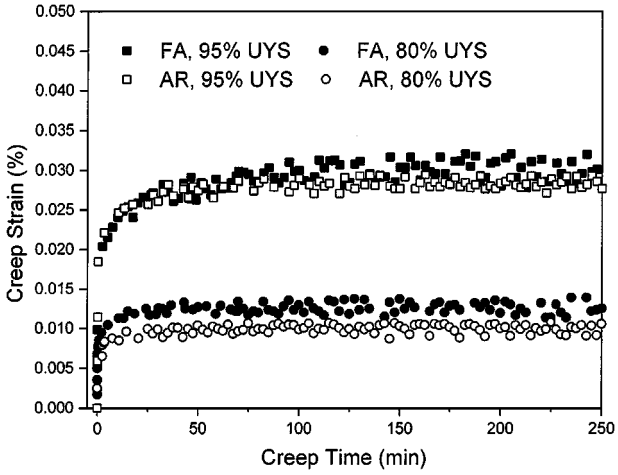

Figure 3 Pre-yield creep curves of the as-received and the annealed X-52 pipeline steels.

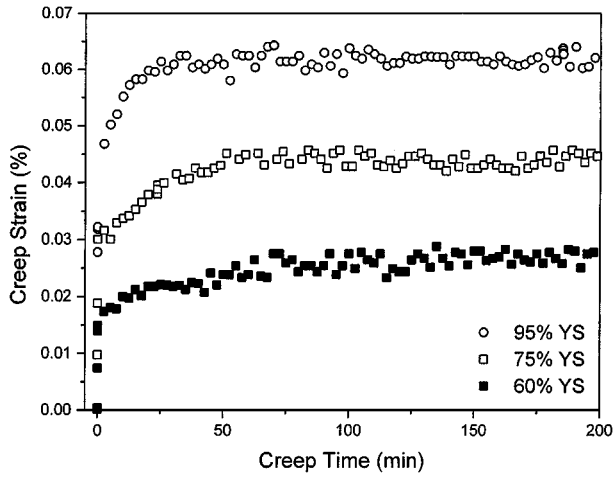

Figure 4 Pre-yield creep curves of the as-received X-70 pipeline steel tested at various stress levels.

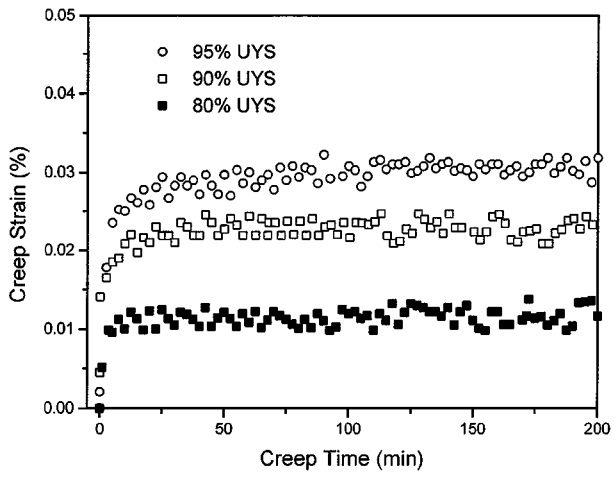

Figure 5 Pre-yield creep curves of the as-received X-80 pipeline steel tested at various stress levels.

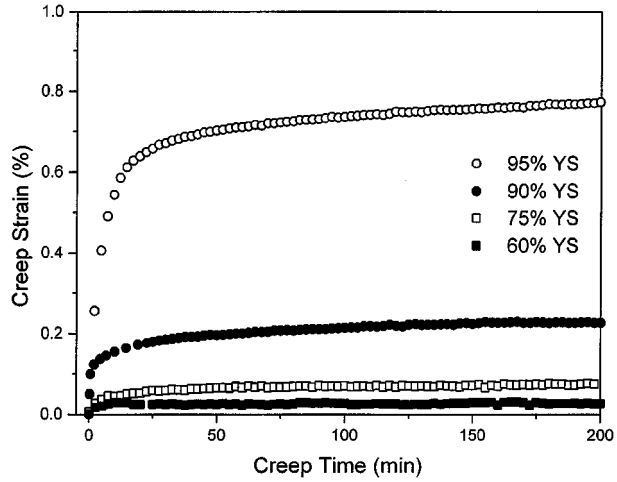

Figure 6 Pre-yield creep curves of the annealed X-70 pipeline steel tested at various stress levels.

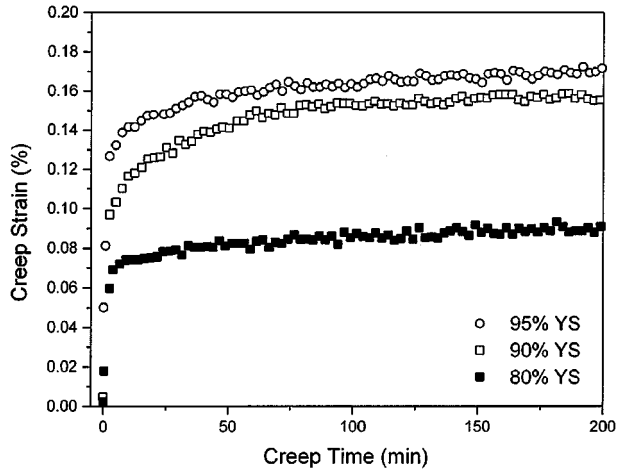

Figure 7 Pre-yield creep curves of the annealed X-80 pipeline steel tested at various stress levels.

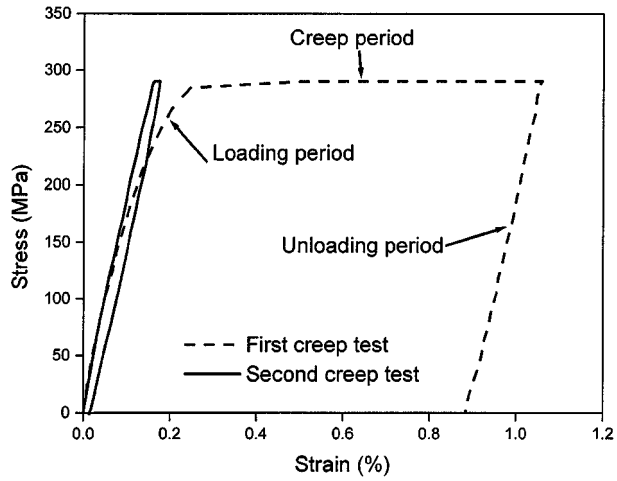

Figure 8 Stress-stain curves of the annealed X-70 steel repeatedly tested under an identical creep stress (95% YS).

which exhibit yield points, the obtained saturated creep stain is significantly smaller than those steels that show a smooth stress-strain curve (Fig. 9). No significant difference in the saturated creep strain can be observed between the as-received and the annealed steels if both of them exhibit a yield point in stress-strain curve (Fig. 3). However, the saturated creep strain is significantly enhanced in the annealed steels that are free of a yield point (compare Fig. 4 with Fig. 6, as well as Fig. 5 with Fig. 7).

As shown in Figs 10 and 11, significant post-yield creep is observed in all the three steels both in the as-received and in the annealed condition. Post-yield creep strain is relatively large even at the condition where

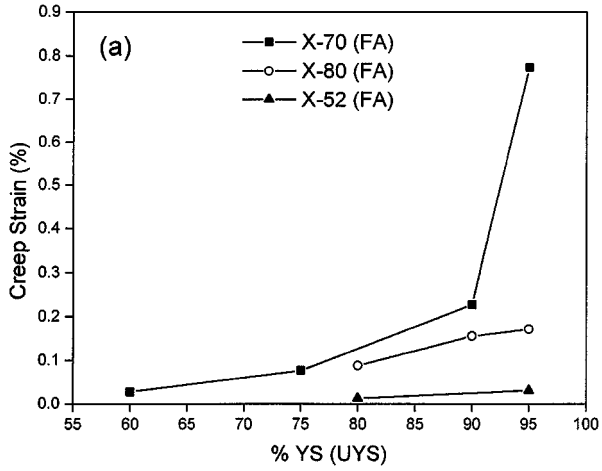

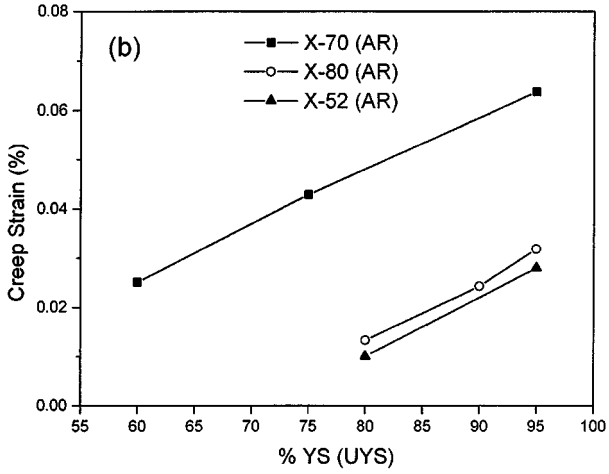

Figure 9 Creep strain up to 200 min as a function of creep stress normalized by the yield strength or the upper yield strength: (a) steels in fully annealed condition; (b) steels in as-received condition.

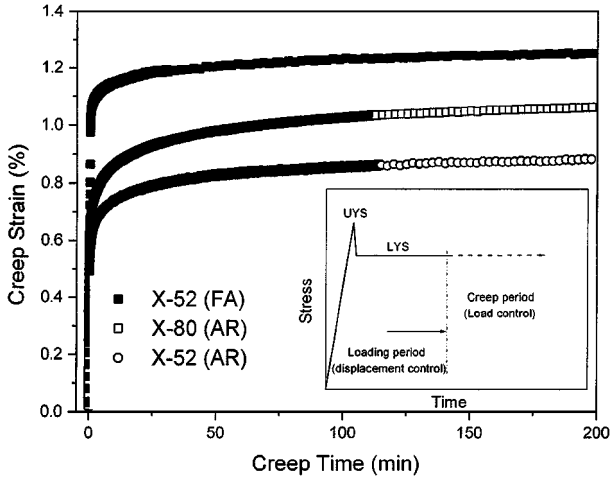

Figure 10 Post-yield creep curves for steels exhibiting yield points. The applied creep stress was equal to the lower yield strength, and initial stain due to loading was controlled to be 1.67% for X52 (AR) and X80 (AR), and 2.78% for X-52 (FA), respectively. The embedded diagram illustrates schematically the loading process.

the creep stress is equal to the lower yield strength (passing the upper yield strength). Nevertheless, the dependence of creep strain on yielding behavior, as seen for the pre-yield creep, is not observed for the post-yield creep. Post-yield creep also exhibits a feature of work-hardening. After creep deformation is exhausted,

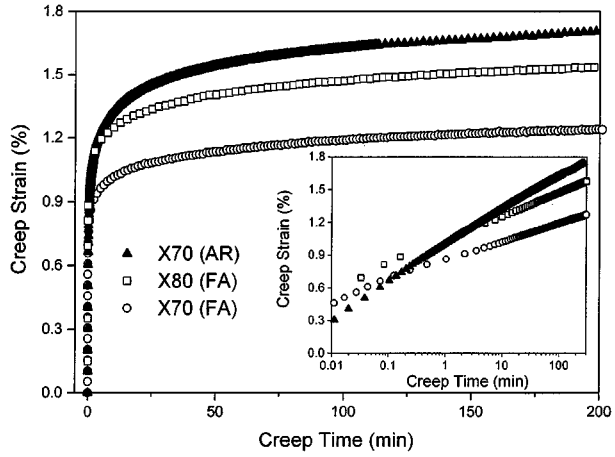

Figure 11 Post-yield creep curves of the as received X-70 tested at 660 MPa, the annealed X-70 tested at 400 MPa, and the annealed X-80 tested at 520. The inserted diagram shows the change of the creep strain with log creep time.

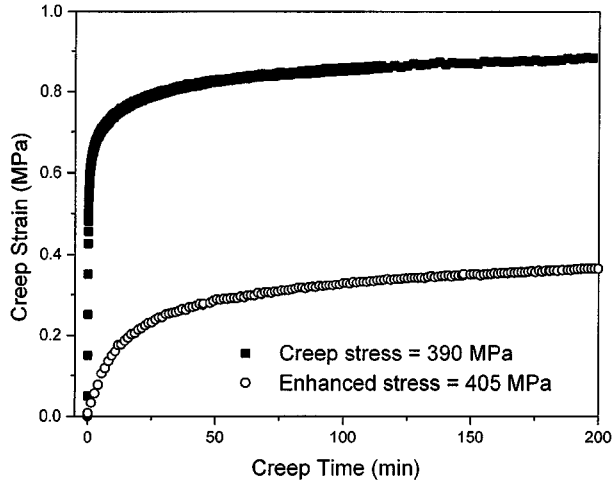

Figure 12 Post-yield creep curves of as-received X-52. The sample was first creep tested at 390 MPa for 200 min, and then experienced a sudden increase in creep stress to 405 MPa.

further creep deformation can be achieved only by increasing the creep stress to a high level, as is shown in Fig. 12. In this figure, the creep strain produced at the new stress level is smaller than that obtained in the first creep test.

4. Discussion

4.1. Stress-strain behavior

A pronounced yield point was observed in both the as-received and the annealed X-52 steels. The presence of yield point is normally attributed either to the dislocation locking [14] or the atmosphere pinning [15] due to the segregation of interstitial elements such as carbon and nitrogen to the dislocation core. TEM characterization has shown that the dislocation density is very low in the as-received X-52 steel (Fig. 13a). This suggests that the carbon and/or nitrogen "atmosphere" formed around dislocation core might be responsible for the observation of yield point in the material. In particular, carbon atmosphere might be dominant since nitrogen in the steel is very low (Table I).

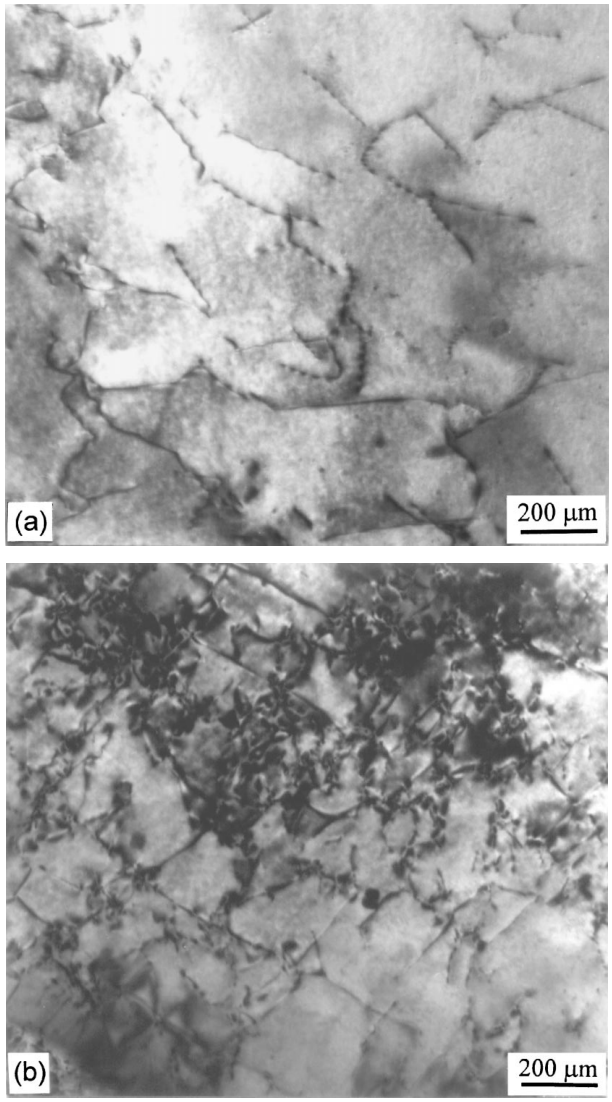

Figure 13 Dislocation structures of the as-received X-52 (a) and the as-received X-80 steel (b).

For the X-80 steel, a yield point was also observed in the as-received condition. However, it has disappeared after the annealing heat treatment. This suggests that the yield behavior in this material might be different from that in the X-52 steel. Although the carbon content is similar in both the steel and the nitrogen content is a little higher in the X-80 steel, the latter steel contains much higher level of alloying elements such as Cb, Mn, Ni and Mo. These elements may have bonded with carbon and/or nitrogen [16, 17] so that fewer interstitial atoms are available to form the "atmosphere" and to lock the dislocations. (Table I). Consequently, the yield phenomenon in the as-received X-80 may be a result of dislocation pinning. This appears consistent with the fact that the as-received X-80 steel is heavily work-hardened with high dislocation density in it (Fig. 13b), and the yield point has disappeared in the fully annealed material.

A yield point was not observed in the as-received X-70 steel, although it has a similar chemistry to the X-80 steel, and both steels were heavily work-hardened in the as-received condition (Fig. 1). This may be attributed to the difference in the dislocation structures present in the steels introduced during fabrication. As shown in Fig. 1, the annealed X-80 steel is much more susceptible to work hardening than the annealed X-70 steel. However, in the as-received state, the X-80 steel had only experienced minor work hardening during tensile testing. This suggests that the as-received X-80 had probably been work-hardened to a much greater extent during fabrication than the as-received X-70. Since it was not fully work-hardened during fabrication, the latter material shows a significant continuing strain hardening during tensile testing. Because of the different degree of work-hardening, the dislocations in as-received X-80 might be mostly mutually locked, and they may become mobile only if the external stress exceeds the locking stress, leading to the presence of a yield point. The same effect was observed in a dual-phase steel by Cimenoglu and Kayali [14]. In contrast, a relatively higher degree of dislocation mobility may exist in the as-received X-70 because of less degree of work-hardening compared to the as-received X-80.

4.2. Creep behavior

The low temperature creep is a consequence of time-dependent dislocation glide [10–12]. According to dislocation dynamics, the creep strain-rate, $\dot{\varepsilon}$, is given by [10–12]

$$\dot{\varepsilon} = \rho_{\mathrm{m}} b v \tag{1}$$

where ρ_{m} is the mobile dislocation density, b the Burgers vector, and v the dislocation velocity. The dislocation velocity is dependent on the effective stress, σ_{e}, acting on the dislocation:

$$v = \left[\frac{\sigma_{\mathrm{e}}}{\tau_0}\right]^n \tag{2}$$

τ_0 is a constant representing the viscous drag to the moving dislocation, n the stress-velocity exponent. The effective stress is given by:

$$\sigma_{\mathrm{e}} = \sigma - \alpha G b \rho_{\mathrm{n}}^{1/2} \tag{3}$$

where σ is the applied stress, G shear Modulus and ρ_{n} the network dislocation density. It is assumed that only the immobile dislocations, which are trapped in dislocation network, will contribute to the hardening of the material and to the reduction of effective stress. At the beginning of creep deformation, the mobile dislocation density is high, resulting in a high creep rate. These mobile dislocations may interact with the dislocation network and become immobilized. As a consequence, the mobile dislocation density will be reduced with time, and the mean distance over which a mobile dislocation can glide will be shortened. Moreover, the increase in network dislocation density will increase the back stress and reduce the effective stress acting on the remaining mobile dislocations (Equation 3). Accordingly, the creep rate (Equation 1) will be reduced with time. The creep strain due to the exhaustion of mobile dislocations normally follows a logarithmic relationship with time [3, 18–21], which has also been observed in this study (Fig. 11).

When the mobile dislocations are exhausted, further deformation can only be produced by increasing the creep stress to a higher level. This high stress may generate new mobile dislocations for deformation. As shown in Fig. 12, the creep strain at the new stress level is far less pronounced than that produced by the initial creep stress, indicating that the mobile dislocation density induced by enhancing the stress is still lower than that during the first creep deformation.

It is intriguing to examine the dependence of pre-yield creep deformation on the materials yielding behavior. While the post-yield creep, to a certain extent, relies on the mobile dislocations generated by the plastic deformation during the period of loading, the pre-yield creep, however, relies mainly on the existing dislocations. For an existing dislocation to become mobile, the applied stress has to be larger than a threshold stress, so that the dislocation is subject to a positive effective stress. According to Equation 3, this threshold stress, σ_{th}, is dependent on network dislocation density:

$$\sigma_{th} = \alpha G b \rho_n^{1/2} \tag{4}$$

In the absence of a yield point, the threshold stress associated with some dislocations may be overcome by a stress below the yield strength. Once the dislocations become mobile, creep deformation occurs.

From Equations 3 and 4, the annealed X-70 and X-80, since they are not work-hardened, should have lower threshold stress and higher effective stress, compared to those the as-received X-70 and X-80. This might be the reason why more creep deformation is produced in the steel with the annealed condition than with the as-received condition (which is especially true for X-70 for which the yield point is absent in both as-received and annealed conditions). As shown in Fig. 9a, the annealed X-70 and X-80 have almost identical creep strain at the creep stress much lower than the yield strength; however, a rapid increase in creep strain in the annealed X-70 was produced when the applied stress was close to the yield strength. This discrepancy may arise from the different work-hardening behavior experienced by these two steels. Much less work-hardening has occurred in the annealed X-70 than in the annealed X-80 (comparing Fig. 2d with 2f).

In the case where the yield point is present, the threshold stress is related to the upper yield strength, below which dislocations are either carbon-locked or "dislocation-locked", so that creep is unlikely to occur, no matter how close the stress level is to the UYS. A very small creep strain observed might be associated with the time-dependent pre-yield microstrain due to the release of some dislocations from the carbon atmospheres (for X-52) or due to dislocation unlocking from the dislocation network (for as-received X-80). In these cases, creep eventually experiences an exhaustion as well. In the former case, for example, the possibilities of such a release become less with increasing time, as dislocations released from the atmosphere exert back stresses reducing local stress at unreleased dislocations [22]. It should be noted that, in the case where the yield point is present, Equation 4 is not valid any more since the critical stress [23] required to separate the dislocation from the atmosphere will be dominant.

4.3. Rate sensitivity of stress-strain behavior

By reviewing the results shown in Fig. 2 and the creep behavior presented above, it is obvious that the stress-strain curve becomes strain-rate sensitive only when a relatively significant creep deformation has occurred. This appears true whether or not the strain-rate sensitivity is observed in the pre-yield region or in the post-yield region. It is known that stress relaxation during tensile testing is often coupled with creep deformation [24]. At lower strain-rate, more time is available for creep-related relaxation. The strain-rate sensitivity may also be explained based on Equations 1–3. In the early stage of plastic deformation, the mobile and network dislocation density may be considered to be similar for a given steel tested at different strain-rates. Higher strain-rate requires a higher dislocation velocity to keep up with the deformation. Since the dislocation velocity is a function of effective stress, a higher stress should be required in order to maintain the strain-rate.

5. Conclusions

1. Dependent on its chemical composition and the processing condition, the pipeline steel may experience different yielding behavior, either with or without yield point. The yield point is present due to a carbon- or dislocation-locking effect on the dislocations.

2. The room temperature creep is controlled by time-dependent dislocation glide. It appears that yielding behavior determines the degree of pre-yield creep deformation. In the presence of a yield point, pre-yield creep occurs only to a minor degree, as dislocations are locked. In the absence of a yield point, the dislocation mobility may be relatively high, and pre-yield creep is likely to occur to a relatively large extent. For the latter case, annealing treatment further enhances creep deformation by increasing the dislocation mobility.

3. Significant post-yield creep exists at room temperature, independent of yielding behavior. The post-yield creep is attributed to the glide of existing dislocations mobilized under the creep stress and new mobile dislocations generated due to plastic deformation in loading process.

4. There is an inherent relationship between strain-rate-sensitivity of stress-strain curve and creep deformation. The effect of strain rate on stress-strain curve could start in the elastic region far below the yield strength as long as there exists significant pre-yield creep deformation.

Acknowledgements

Thanks are due to professor M. C. Chaturvedi, Department of Mechanical & Industrial Engineering, University of Manitoba, for the use of the transmission electron microscope in his laboratory. The authors would also like to thank the Natural Science and Engineering

Research Council of Canada and the TransCanada Pipeline Ltd. for financial support.

References

1. Z. ZHAO, D. O. NORTHWOOD, C. LIU and Y. LIU, *Journal of Materials Processing Technology* **89/90** (1999) 569.
2. R. N. PARKINS, in "Stress Corrosion Cracking—The Slow Strain-Rate Technique," ASTM STP 665, edited by G. M. Ugiansky and J. H. Payer (American Society for Testing and Materials, Philadelphia, 1979) p. 5.
3. A. OEHLERT and A. ATRENS, *Acta Metall. Mater.* **42** (1994) 1493.
4. *Idem.*, in "Parkings Symposium on Fundamental Aspects of Stress Corrosion Cracking," edited by S. M. Bruemmer *et al.* (The Minerals, Metals & Materials Society, 1992) p. 255.
5. M. M. FESTEN, J. G. ERLINGS and R. A. FRANSZ, in Proc. First Int'l. Conf. on Environment-Induced Cracking of Metals, Oct. 2–7, 1988 (NACE, Houston) p. 229.
6. K. ISHIKAWA, H. OKUDA, M. MAEHARA and Y. KOBAYASHI, in Experimental Mechanics, edited by Allison (Balkema, Rotterdam, 1998) p. 1349.
7. K. ISHIKAWA, H. OKUDA and Y. KOBAYASHI, *J. Mater. Sci. Lett.* **17** (1998) 423.
8. W. K. MILLER, *Metall. Trans. A* **22A** (1991) 873.
9. W. H. MILLER, R. T. CHEN and E. A. STARKE, *ibid.* **18A** (1987) 1451.
10. T. H. ALDEN, *ibid.* **18A** (1987) 51.
11. *Idem., ibid.* **18A** (1987) 811.
12. *Idem., ibid.* **16A** (1985) 375.
13. Z. A. YANG, Z. G. WANG and S. Q. WANG, *Mater. Sci. Eng. A* **102** (1988) 17.
14. H. CIMENOGLU and E. S. KAYALI, *Scripta Metall. Mater.* **24** (1990) 2437.
15. F. R. N. NABARRO, "Theory of Crystal Dislocations" (Oxford University Press, London, 1967).
16. J. P. NAYLOR and M. GUTTMANN, *Met. Sci.* **15** (1981) 433.
17. S. D. MANN and B. C. MUDDLE, *Mater. Sci. Tech.* **13** (1997) 299.
18. E. H. JORDAN and A. D. FRED, *Exp. Mech.* **22** (1982) 354.
19. D. UCHIC and W. D. NIX, *Mat. Res. Soc. Symp. Proc.* **460** (1997) 437.
20. T. OGATA, O. UMEZAWA and K. ISHIKAWA, *Advances in Cryogenic Engineering (Materials)* **36** (1990) 1233.
21. R. DUTTON, "A Review of the Low-Temperature Creep Behaviour of Titanium," AECL-11544, COG-96-70-I, Whiteshell Laboratories, Pinawa, Manitoba, Canada, 1996.
22. D. S. WOOD, in "Dislocations and Mechanical Properties of Crystals," edited by J. C. Fisher *et al.* (John Wiley & Sons, New York, 1957) 413.
23. D. HULL, "Introduction to Dislocations" (Pergamon Press, Oxford, 1965).
24. C. Y. JEONG, S. W. NAM and J. GINSZTLER, *J. Mater. Sci.* **34** (1999) 2513.

Received 10 March
and accepted 18 September 2000